

GAS-PHASE PHOTOCATALYZED ACETONE OXIDATION

Jaime JIMÉNEZ-BECERRIL¹, Xavier DOMÈNECH² and José PERAL^{2*}

¹Departamento de Química, Instituto Nacional de Investigaciones Nucleares, Apartado Postal 18-1027, D.F. 11801 México

²Departament de Química, Edifici Cn, Universitat Autònoma de Barcelona, 08193 Bellaterra (Barcelona), Spain

(Recibido diciembre 1997, aceptado noviembre 1998)

Keywords: acetone, gas-phase, photocatalysis, TiO₂

ABSTRACT

The gas-phase acetone oxidation catalyzed by photoexcited semiconductors was studied. The influence of different experimental parameters like light intensity, water concentration in the gas phase, temperature and acetone concentration on the oxidation process were determined. Quantification of acetone adsorption without light and detection of CO₂ upon irradiation, the main indicator of mineralization, were also verified. Most experiments were carried out using anatase TiO₂ as catalyst, although other semiconductors like rutile TiO₂, ZnO, Fe₂O₃, CdS and WO₃ were tested. TiO₂ anatase was found to be the only one capable of inducing mineralization.

RESUMEN

Se estudió la oxidación de la acetona en fase gaseosa mediante catalizadores semiconductores fotoexcitados. En particular, se siguió la influencia de diferentes parámetros experimentales, como intensidad de luz incidente, concentración de agua en fase gaseosa, temperatura y concentración de acetona, sobre el proceso de oxidación. También se cuantificaron la adsorción de acetona en oscuridad y la formación de CO₂ como producto final de la reacción y como índice del grado de mineralización. La mayoría de los experimentos fueron realizados utilizando TiO₂ como catalizador, aunque también se probaron otros semiconductores como TiO₂ rutilo, ZnO, Fe₂O₃, CdS y WO₃, observándose que sólo el TiO₂ anatasa era capaz de producir mineralización.

INTRODUCTION

Factory and building air standards frequently involve low ambient pollutant levels. Air quality problems may concern odors, which are also due to the presence of chemical species at low concentration levels. The removal of these contaminants and the remediation of mildly polluted closed atmosphere has been traditionally carried out by means of porous carbon adsorbers, which are not a desirable solution to the problem, since they have to be periodically replaced. The pollutant is removed, but not destroyed, and the operation generates new environmentally undesirable effects.

The biological treatment of polluted closed atmospheres is also inadequate. The microorganisms need almost 100% humidity levels in order to perform their task. This is a clearly unacceptable condition to sustain human respiration.

Thermocatalytic treatment of contaminated or polluted air or combustion gases is a well established technique in which the application of catalytic exhaust oxidation/reduction catalysts, catalytic incineration, and catalytic combustion are usually employed. These processes require temperatures of 200 to 900 °C, they involve oxidizable species in concentrations of several hundreds of ppm, and are not economically advisable to remove lower pollutant concentrations (Satterfield 1991). The need for a low ambient temperature catalytic oxidation system which can carry out complete destruction of oxidizable contaminants is evident.

Gas-phase heterogeneous photocatalysis is an oxidation technique which could be successfully used for this purpose (Fu *et al.* 1996, Peral *et al.* 1997). A photoactive semiconductor, usually a metal oxide like TiO₂, ZnO, Fe₂O₃, etc., can absorb light in the UV-visible zone generating electron-hole pairs

*Author to whom correspondence should be addressed

which, after migrating to the catalyst surface, can promote electron transfer reactions and create the conditions needed for an effective destruction of almost any type of organic species in contact with the heterogeneous interface. Liquid-phase photocatalysis has been widely studied and is now at the application level; water treatment photocatalytic reactors are already available (Hoffman *et al.* 1995). Gas-phase studies have been fewer, but their potential use to remediate contaminated closed atmospheres is considerable. In the present paper different mixtures of acetone in air were used to study the TiO_2 -assisted gas-phase photocatalytic oxidation of acetone as a model of organic compounds. Data from different experimental conditions are presented and the performance of a series of potential catalysts are also considered.

MATERIALS AND METHODS

Figure 1 shows a schem of the experimental system used for the photocatalytic studies. An UHP air tank (A) was used to provide a continuous air stream through the system. Using the appropriate set of valves (v), "T" connections and the flow sensor-controllers (MFC1, MFC2 and MFC3) (Bronkhost Hi-Tec) coupled to a mass flow controller unit, three secondary air streams were obtained. Mass flow sensors MFC1 and MFC2 could supply a maximum of $500 \text{ cm}^3 \text{ min}^{-1}$ of air. The third one (MFC3) supplied $20 \text{ cm}^3 \text{ min}^{-1}$ and its air stream was bubbled through liquid acetone at constant temperature (AS), producing a mixture of air-acetone of uniform composition. The air stream of one of the $500 \text{ cm}^3 \text{ min}^{-1}$ mass flow sensors (MFC2) was used to introduce the water vapor into the system, and to bubble air through liquid water (WS). By changing the three different flows and the sparging temperatures a broad range of acetone and water vapor concentration could be fed into the photoreactor (R) or led to chromatographic analysis (GC) with an appropriated bypass.

The photoreactor was a cylindrical vessel (6 cm high and 4.15 cm^2 base) with an interior, attached fritted glass plate used to support the powdered photocatalyst and through which the downward flow passed. An air-tight quartz window enclosed the reactor top. Two lateral ports provided the sampling site and the inlet of the gas mixture, being the outlet port beneath the fritted glass plate.

The vapor samples were analyzed by gas chromatography (Varian Star 3400 cx) operating with a TCD detector and a Poropack Q column (100/120 support in a $2 \text{ m} \times 1/8''$ SS tube). Using a temperature ramp (1 min at 100°C and rising to 200°C at $30^\circ\text{C min}^{-1}$) four GC peaks could be detected: air (0.38 min), CO_2 (0.75 min), H_2O (2.19 min), and acetone (4.98 min).

The catalysts were used as supplied without pretreatment. The characteristic of the different catalysts were as follows: a) Anatase TiO_2 Degussa P25, with a primary particle diameter of 30 nm and a surface area of $50 \text{ m}^2 \cdot \text{g}^{-1}$. The P25 particles were spherical and nonporous, with a state purity of $> 99.5\%$ TiO_2 ; b) Rutile TiO_2 Aldrich with a particle diameter of 500 nm and 19.7

$\text{m}^2 \cdot \text{g}^{-1}$ of surface area; c) ZnO Probus with a particle diameter of 400 nm and $34.6 \text{ m}^2 \cdot \text{g}^{-1}$ of surface area; d) $\alpha\text{-Fe}_2\text{O}_3$ Merck; e) WO_3 Merck with a particle diameter of 500 nm; and f) CdS Scharlau with a particle diameter of 400 nm. The acetone used to prepare the gas mixtures was of HPLC grade, supplied by Aldrich.

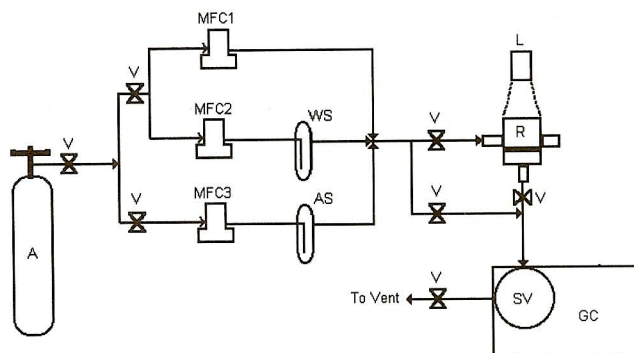


Fig. 1. Schem of the experimental system used for the photocatalytic studies. A = UHP air tank; V = valves; MFC = mass flow controllers; WS = water saturator; AS = acetone saturator; L = light source; R = photochemical reactor; SV = six ports sampling valve; and GC = gas chromatograph

The light source was a 80 W medium pressure Hg lamp (Frielite MB). To prevent any true UV (200–300 nm) homogeneous photoreaction, a Pyrex plate was positioned over the reactor window to absorb the incident radiation having $\lambda < 300 \text{ nm}$ and to transmit only the near-UV light for the catalyst photoactivation. The lamp power output detected at the top of the reactor with a NRC 820 Laser Power Meter working at 514 nm was $0.3 \mu\text{W} \cdot \text{cm}^{-2}$.

In a typical experiment, 0.15 g of catalyst powder were spread uniformly over the surface of the porous fritted glass plate. With the only slightly contaminated air feed, the surface inventory of strongly held reactant required some time to accumulate to a "dark" gas-solid equilibrium. Consequently, the trace contaminated air had to be fed first for a considerable period of time (typically 60–90 min) until the feed and reactor exit gas concentrations were identical (no "dark" reaction products were noted). When that condition was achieved, the reactor was closed, the gas flow shut down and the light turned on, and gas samples were taken periodically with a gas-tight syringe for GC injections.

RESULTS AND DISCUSSION

A preliminary quantification of the amount of acetone adsorbed onto the TiO_2 catalyst in the dark was carried out. 0.15 g of TiO_2 anatase were placed on the fritted glass plate and a continuous flow of $37 \text{ ml} \cdot \text{min}^{-1}$ of a $2.15 \cdot 10^5 \text{ ppmv}$ air-acetone

mixture was forced to pass through the reactor. The acetone concentration was sequentially measured (Fig. 2), and the resulting data showed a large initial acetone adsorption which decreased with time. After approximately 250 min the catalyst surface was acetone saturated with $1.74 \cdot 10^{-3} \text{ mol g TiO}_2^{-1}$. This number is at least one order of magnitude higher than the values previously reported ($1.7 \cdot 10^{-4} \text{ mol g TiO}_2^{-1}$ (Raupp *et al.* 1993) and $4.4 \cdot 10^{-5} \text{ mol g TiO}_2^{-1}$ (Peral *et al.* 1992), which indicates that surface coverage is in equilibrium with the more concentrated feed of acetone used in these experiments.

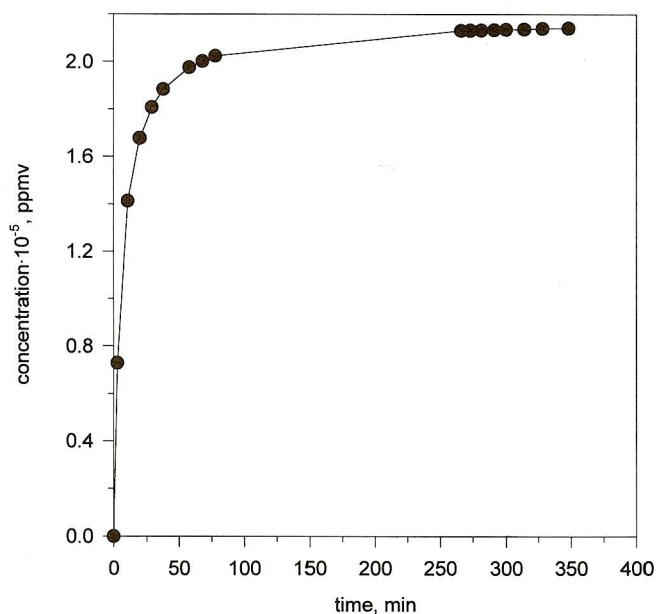


Fig. 2. Outlet reactor acetone concentration vs. flow time. Acetone concentration $2.15 \cdot 10^5 \text{ ppmv}$. Mass of TiO_2 0.15 mg. Gas flow $37 \text{ ml} \cdot \text{min}^{-1}$

The photocatalytic activity of TiO_2 toward the destruction of acetone is illustrated with the batch reactor data shown in figure 3. A $3 \cdot 10^4 \text{ ppmv}$ acetone-air mixture was allowed to flow through the fritted glass during 90 minutes and following surface catalyst saturation the reactor was closed and the light turned on. A regular decrease of acetone concentration vs. irradiation time is observed, being this a repetitive behavior in two different experiments. Simultaneously, a small GC peak of CO_2 which increased with irradiation time was detected. Therefore, mineralization to CO_2 seems to be the final sink of the acetone that was removed from the gas mixture.

The dependence of photocatalytic reaction yield on light intensity was studied. In previous research it was found that, for liquid phase photocatalysis at very low intensities (less than one sun near-UV equivalent), first order dependence takes place (Egerton *et al.* 1979, Okamoto *et al.* 1985), whereas at above one sun near-UV equivalent, half order applies (D'Oleivera *et al.* 1990, Kormann *et al.* 1991). Figure 4 includes data corresponding to gas-phase acetone photooxidation at

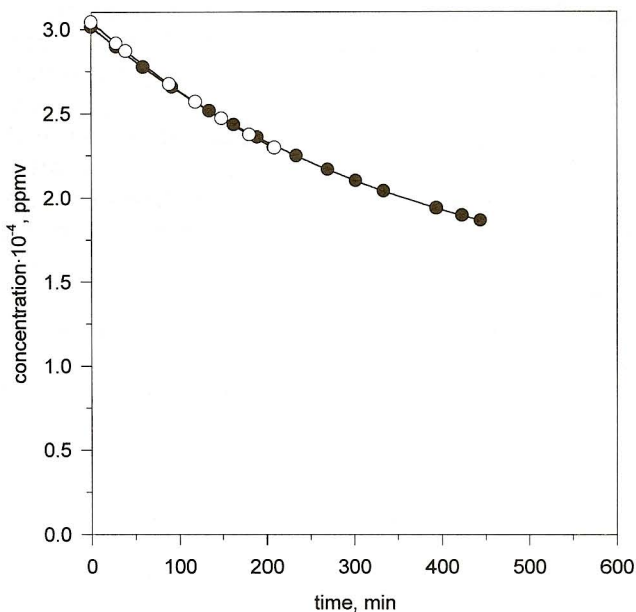


Fig. 3. Batch reactor data of the change of acetone concentration vs. irradiation time. Data from two experiments (O and ●) carried out under the same experimental conditions: $[\text{acetone}]_0 = 3 \cdot 10^4 \text{ ppmv}$; $[\text{H}_2\text{O}]_0 = 2.26 \cdot 10^5 \text{ ppmv}$; mass of $\text{TiO}_2 = 0.15 \text{ g}$

different light intensities. The experiments were carried out with the reactor working in batch mode and using TiO_2 as catalyst. As it can be seen, after an initial transient behavior, the four different intensities exhibit a steady removal of acetone, the rate being almost the same in the four cases (31 ppmv min^{-1}),

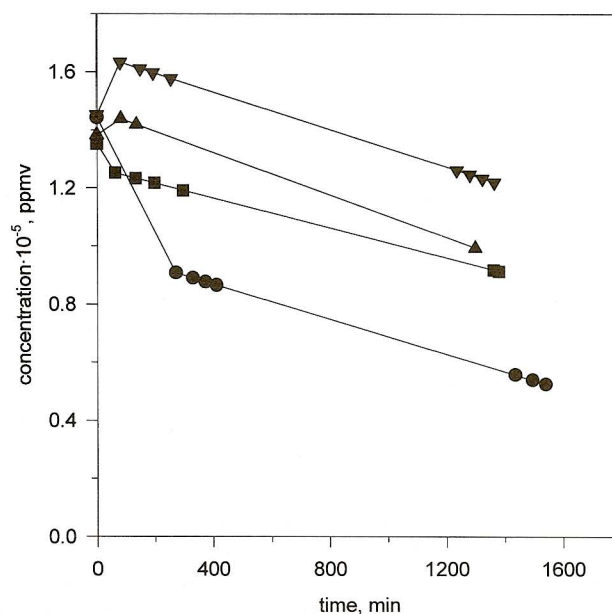


Fig. 4. Dependence of acetone concentration and relative light intensity: (▼) 100%, (▲) 55%, (■) 46% and (●) 32% of the total lamp power output ($0.3 \mu\text{W} \cdot \text{cm}^{-2}$). $[\text{acetone}]_0 = 1.4 \cdot 10^5 \text{ ppmv}$; $[\text{H}_2\text{O}]_0 = 2.26 \cdot 10^5 \text{ ppmv}$; mass of $\text{TiO}_2 = 0.15 \text{ g}$

which indicates that under the experimental conditions tested, the catalytic reaction rate is not photon-controlled. However, the initial reaction transient (first 150–200 minutes) is clearly intensity dependent. An initial increase of acetone concentration takes place for the two larger photon fluxes, evidencing the existence of a photo-assisted desorption as consequence of a TiO_2 surface change upon irradiation. The fact that semiconductor surface properties and adsorption equilibrium change during irradiation has been previously noticed (Baidyaroy *et al.* 1971, Munuera *et al.* 1971). The initial acetone desorption is changed into adsorption for the two lower light intensities, indicating that more TiO_2 surface active sites are generated upon mild irradiation.

Water concentration in the gas flow is also an important variable which could influence the gas-phase photocatalytic reaction (Bickley *et al.* 1973, Dibble *et al.* 1990). In principle, two different effects can be related to the presence of water (Peral *et al.* 1997): i) oxidation failure occurs in absence of water since it is needed for the stoichiometric oxidation of acetone, and ii) water can inhibit the reaction due to its role as competitor for the surface active sites. Consequently, water in low concentrations seems to be essential for the sustainability of the reaction, but this can be precluded when the concentration rises. Several gas-phase humidities were tested in order to identify such water dependencies while photooxidizing acetone. Figure 5 depicts the change in acetone concentration with irradiation time for the three different water loads. As can be seen, the reaction rate of the less humid condition (slope of curve with \blacktriangle data points) is the fastest one and it decreases with increasing amounts of water. However, a transient behavior is observed during the first 50 minutes where the initial acetone

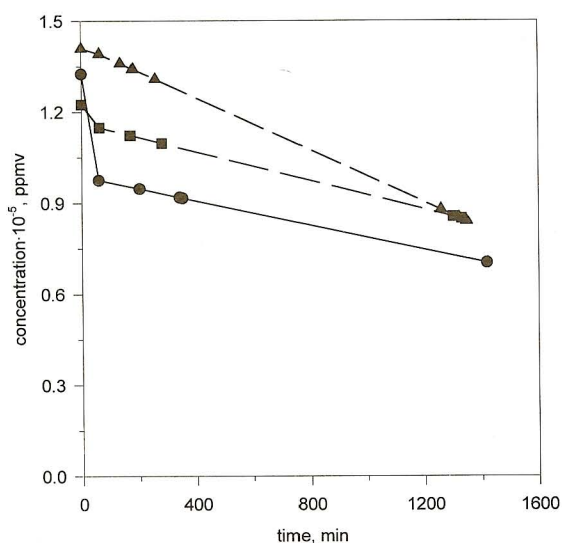


Fig. 5. Effect of water load on the photocatalytic reaction yield. (●) $2.26 \cdot 10^5$ ppmv of water and $1.32 \cdot 10^5$ ppmv of acetone ($[\text{H}_2\text{O}]/[\text{Acetone}] = 1.712$), (■) $4.39 \cdot 10^4$ ppmv of water and $1.22 \cdot 10^5$ ppmv of acetone ($[\text{H}_2\text{O}]/[\text{Acetone}] = 0.359$), and (▲) $2.92 \cdot 10^4$ ppmv of water and $1.39 \cdot 10^5$ ppmv of acetone ($[\text{H}_2\text{O}]/[\text{Acetone}] = 0.210$);

removal is faster in the more humid samples.

This fact can be rationalized in terms of a larger $\text{HO}\cdot$ production along with higher acetone surface coverage at the beginning of the reaction. Depletion of adsorbed acetone due to larger water coverages would cause the reaction rate reduction observed at longer reaction times. In fact, a wider range of water concentrations should have been tested since different behaviors could have been observed at more or less water loaded mixtures.

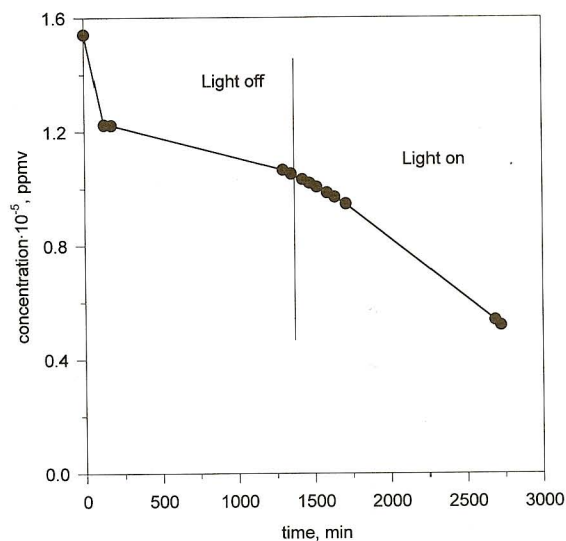


Fig. 6. Effect of temperature on acetone oxidation. $[\text{acetone}]_0 = 1.51 \cdot 10^5$ ppmv, $[\text{H}_2\text{O}]_0 = 2.26 \cdot 10^5$ ppmv, mass of $\text{TiO}_2 = 0.15$ g

The majority of heterogeneous photocatalytic reactions have been carried out at ambient temperature. Slight increase of reaction rate have been reported in liquid phase, with Arrhenius behavior and activation energies which agree well with those found for $\text{HO}\cdot$ radical reactions (Fox *et al.* 1993). A more complicated situation is expected for gas-phase systems where temperature strongly affects both the adsorption-desorption equilibrium and the reaction kinetics. In our study, acetone oxidation was also tested at 80°C and the data are shown in figure 6 where removal of acetone vs. reaction time is plotted both in the dark and under irradiation. TiO_2 was the catalyst used for the treatment of the $1.51 \cdot 10^5$ ppmv acetone-air mixture in the batch-mode reactor. As can be seen, acetone is clearly removed even in the absence of light. This fact can be explain in terms of a thermocatalytic decomposition without complete mineralization since CO_2 was not detected. It is also clear from the change of slope that light further increases the acetone destruction. CO_2 was detected at the outlet of the reactor only in presence of light, which indicates complete mineralization of acetone. Thus light and thermal activation are both effective in term of acetone removal but only light activation can cause complete mineralization.

Acetone oxidation was also studied at different initial concentrations ranging from $1.22 \cdot 10^4$ ppmv to $2.6 \cdot 10^5$ ppmv, as

shown in **figure 7**. The resulting data were adjusted using the Langmuir-Hinshelwood (L-H) kinetic model which considers that the chemical reaction is the rate limiting step and adsorption-desorption of acetone is in equilibrium and follows a Langmuir adsorption isotherm. The L-H equation is (Ollis *et al.* 1989):

$$r = \frac{-d[\text{acetone}]}{dt} = \frac{kK[\text{acetone}]}{1 + K[\text{acetone}]}$$

being k the reaction rate constant and K the adsorption-desorption equilibrium constant. The inverse of this equation is a linear relation between $1/r$ and $1/[\text{acetone}]$, which has to be in good agreement with the experimental data. In order to avoid long term unexpected processes to interfere the fitting, only initial reaction rates were considered. The insert in **figure 7** shows a good linear fitting indicating that the reaction follows the L-H kinetics. The values found for k and K were $140 \text{ ppmv min}^{-1}$ and $2.5 \cdot 10^{-6} \text{ ppmv}$, although it has to be said that the reliability of these quantities is fairly low due to their strong dependence on slope and y-axis intercept.

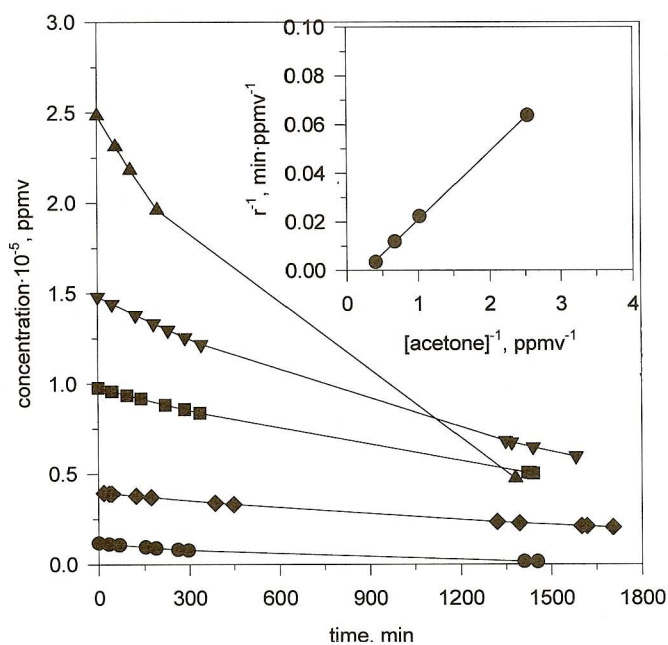


Fig. 7. Acetone concentration vs. irradiation time for different initial concentrations: (●) 12200 ppmv, (◆) 39100 ppmv, (■) 97800 ppmv, (▼) 147000 ppmv, and (▲) 260000 ppmv. $[\text{H}_2\text{O}]_0 = 2.26 \cdot 10^5 \text{ ppmv}$, mass of $\text{TiO}_2 = 0.15 \text{ g}$. The insert shows the linear fitting between r^{-1} and $[\text{acetone}]^{-1}$. The rates were calculated only considering data point for the first 300 minutes

Finally, other materials apart from TiO_2 anatase were tested as effective gas-phase acetone photocatalysts. The election was based on material semiconducting properties and previous experience collected in liquid phase studies. **Figure 8** shows the changes in acetone concentration obtained with irradiation time for TiO_2 anatase, TiO_2 rutile, Fe_2O_3 , WO_3 , CdS and ZnO . As can be seen, when using Fe_2O_3 and ZnO acetone removal is improved

with regard to the use of TiO_2 anatase. However, no CO_2 was detected in those two cases, indicating that acetone decrease was produced by surface adsorption. Furthermore, CO_2 was neither detected for the rest of the catalysts, TiO_2 anatase proving to be the only one among the different choices to promote acetone mineralization. This fact along with other material properties like chemical stability, lack of photo-corrosion, and innocuous character emphasize the suitability of TiO_2 anatase as photocatalyst for the destruction of low concentration organic polluted atmospheres.

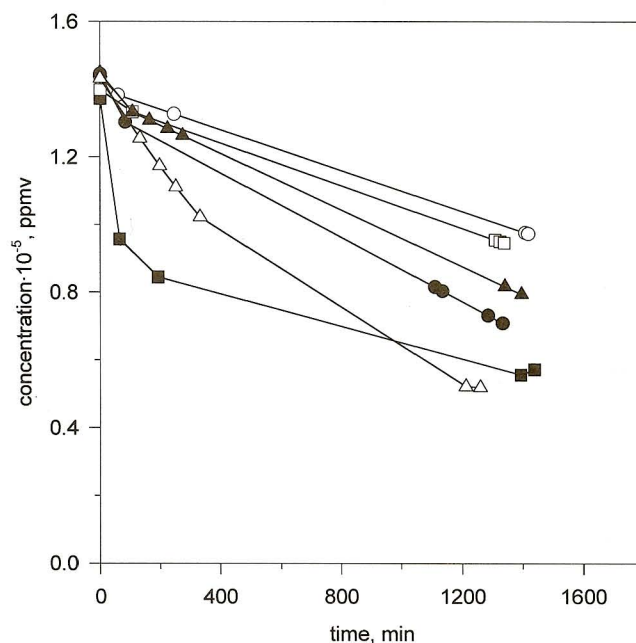


Fig. 8. Acetone concentration vs. irradiation of several semiconducting materials: (●) TiO_2 anatase, (○) TiO_2 rutile, (□) WO_3 , (▲) CdS , (■) Fe_2O_3 , and (△) ZnO . $[\text{H}_2\text{O}]_0 = 2.26 \cdot 10^5 \text{ ppmv}$, mass of catalyst = 0.15 g

CONCLUSIONS

TiO_2 assisted photocatalytic oxidation of mixtures of acetone and air has been carried out, showing complete mineralization of the organic matter to CO_2 . Decrease of acetone concentration in the absence of near UV light takes place mainly due to dark adsorption onto the catalyst surface. Thermal removal of acetone (80°C) has also been observed, although CO_2 formation again required the presence of light. No dependence of the reaction rate on different photon intensities has been found, but some evidence points toward the existence of an initial photo-assisted desorption of acetone as consequence of a TiO_2 surface properties change upon irradiation. Water vapor concentration in the gas mixture has shown to initially favor the photocatalytic process, but increasing water contents decrease the rate of acetone removal

at longer reaction times. The kinetics of acetone oxidation obeys a Langmuir-Hinshelwood rate law, and first order reaction rate and adsorption equilibrium constants have been reported. Finally, other catalysts, like TiO_2 rutile, WO_3 , CdS , Fe_2O_3 and ZnO were tested for the photooxidation of acetone, although none of them were able to accomplish total mineralization and generation of CO_2 . The TiO_2 assisted photocatalytic destruction of organics at room temperature seems a promising technology for the remediation of mildly polluted enclosed atmospheres.

ACKNOWLEDGEMENTS

The authors thank the CICYT, Spain (Project AMB96-0742) and CONACyT (Mexico) for the financial support of Dr. Jaime Jiménez.

REFERENCES

- Baidyaroy S., Bottoms W.R. and Mark P. (1971). Photodesorption from CdS . *Surf. Sci.* 28, 517-524.
- Bickley R.I. and Stone F.S. (1973). Photoadsorption and photocatalysis at rutile surfaces I. Photoadsorption of oxygen. *J. Catal.* 31, 389-397.
- Dibble L.A. and Raupp G.B. (1990). Kinetics of gas-solid heterogeneous photocatalytic oxidation of trichloroethylene by near-UV illuminated titanium dioxide. *Catal. Letters*, 4, 345-354.
- D'Oleivera J., Al-Sayyed G. and Pichat P. (1990). Photodegradation of 2- and 3-chlorophenol in titanium dioxide aqueous suspension. *Environ. Sci. Technol.* 25, 990-997.
- Egerton T.A. and King C.J. (1979). The influence of light intensity on photoactivity in titanium dioxide pigmented systems. *J. Oil Col. Chem. Assoc.* 62, 386-389.
- Fox M.A. and Dulay M.T. (1993). Heterogeneous photocatalysis. *Chem. Rev.* 93, 341-357.
- Fu X., Zeltner W.A. and Anderson M.A. (1996). Applications in photocatalytic purification of air. In: *Semiconductor Nanoclusters* (P.V. Kamat and D. Meisel, Eds.). Studies in Surface Science and Catalysis, Vol. 103, Elsevier Science, Amsterdam, pp. 445-461.
- Hoffmann M.R., Martin S.T., Choi W. and Bahnemann D.W. (1995). Environmental applications of semiconductor photocatalysis. *Chem. Rev.* 95, 69-96.
- Kormann C., Bahnemann D.W. and Hoffmann M.R. (1991). Photolysis of chloroform and other organic molecules in aqueous TiO_2 suspensions. *Environ. Sci. Technol.* 25, 494-500.
- Munuera G. and Stone F.S. (1971). Adsorption of water and organic vapours on hydroxilated rutile. *Discuss. Faraday Soc.* 52, 205-214.
- Okamoto K., Ysamamoto Y., Tanaka H. and Itaya A. (1985). Kinetics of heterogeneous photocatalytic decomposition of phenol over anatase TiO_2 powder. *Bull. Chem. Soc. Japan* 58, 2023-2028.
- Ollis D.F., Pelizzetti E. and Serpone N. (1989). Heterogeneous photocatalysis in the environment: application to water purification. In: *Photocatalysis fundamentals and application* (N. Serpone and E. Pelizzetti, Eds.). Wiley, New York, pp. 603-637.
- Peral J. and Ollis D.F. (1992). Heterogeneous photocatalytic oxidation of gas-phase organics for air purification: acetone, 1-butanol, butyraldehyde, formaldehyde and m-xylene oxidation. *J. Catal.* 136, 554-565.
- Peral J., Domènech X. and Ollis D.F. (1997). Heterogeneous photocatalysis for purification, decontamination and deodorization of air. *J. Chem. Technol. Biotechnol.* 70, 117-140.
- Raupp G.B. and Junio C.T. (1993). Photocatalytic oxidation of oxygenated air toxics. *Appl. Surf. Sci.* 72, 321-327.
- Satterfield C.N. (1991). *Heterogeneous catalysis in industrial practice*. Mc Graw-Hill, New York.